International Journal of Power Electronics and Drive System (IJPEDS)
Vol. 17, No. 2, June 2026, pp. 933∼945
ISSN: 2088-8694, DOI: 10.11591/ijpeds.v17.i2.pp933-945

Improved control strategy for harmonic current mitigation in DFIG-based wind turbines supplying linear and nonlinear loads

Hind Elaimani, Noureddine Elmouhi
Laboratory of Innovation in Management and Engineering, Edvantis Higher Education Group, ISGA, Rabat, Morocco

Article Info

Article history:

Received Sep 8, 2025
Revised Mar 8, 2026
Accepted Apr 23, 2026

Keywords:

Active filter
DFIG
Harmonic mitigation
Sliding mode
THD

ABSTRACT

Improving power quality is a major challenge in grid-connected wind energy systems, especially under mixed linear and nonlinear load conditions. This paper proposes an enhanced control strategy for harmonic current mitigation in a doubly fed induction generator (DFIG)-based wind turbine. The proposed approach integrates flux-oriented vector control with an active harmonic compensation algorithm implemented through the rotor-side converter (RSC). Unlike conventional methods that target only specific harmonic orders, the proposed strategy mitigates all current harmonics at the point of common coupling (PCC). Simulation studies conducted under various load conditions demonstrate that the method significantly reduces the total harmonic distortion (THD) and ensures near-sinusoidal stator currents. The results confirm the effectiveness and robustness of the proposed control approach in improving the power quality of DFIG-based wind energy conversion systems.

Corresponding Author:

Hind Elaimani
Laboratory of Innovation in Management and Engineering, Edvantis Higher Education Group, ISGA
27, Avenue Oqba, 27 Av. Oqba Ibn Naafi, Rabat 10090, Morocco
Email: h.elaimani@gmail.com

1. INTRODUCTION

In recent decades, the global demand for electrical energy has increased rapidly due to industrialization and the widespread use of electrical appliances [1], [2]. To meet this growing demand while reducing environmental impact, many countries are integrating renewable energy sources into their power systems, with wind energy emerging as a prominent option due to its high potential and reliability. Several recent studies have investigated harmonic mitigation in renewable energy systems. A first work [3] implemented a unified power quality conditioner (UPQC) combining series and shunt active filters to reduce current and voltage distortions, achieving a decrease in total harmonic distortion (THD) from over 55% to less than 5%. Another study [4] explored reactive power control on the grid-side converter of a wave energy system to attenuate voltage harmonics. A comprehensive review [5] has also discussed the use of inverter-based distributed generation units as active power quality conditioners for harmonic compensation. Moreover, research involving indirect current control (ICC) combined with fuzzy logic control (FLC) demonstrated effective harmonic reduction under highly nonlinear loads, maintaining compliance with IEEE 519-1992 standards [6]. Finally, studies on DFIG-based wind turbines have critically analyzed harmonic reduction methods to enhance the quality of the current injected into the grid [7]. Together, these works highlight the need for more integrated and adaptive strategies capable of addressing complex harmonic profiles in renewable energy systems. Among

various generator configurations for wind energy conversion, doubly fed induction generators (DFIGs) are widely employed because of their efficiency and controllability. Several control strategies have been developed, including sliding mode control, which offers fast response and high precision [8]–[10]. Modern wind energy systems are expected not only to deliver active power but also to provide ancillary services such as reactive power support and harmonic current mitigation. Voltage fluctuations and harmonic distortions can disrupt sensitive equipment and degrade power quality, quantified by THD [11]. Numerous methods have been proposed to reduce harmonics, including modified rotor-side converter (RSC) control, grid-side converter (GSC) adjustments, and external active filters [2], [12]–[17]. Despite these advances, a comprehensive strategy capable of suppressing all harmonic components while maintaining the main objectives of the wind energy conversion system (active power generation and reactive power compensation) is still lacking. To address this gap, this study proposes a harmonic mitigation strategy integrating a multivariable filter with sliding mode control of both RSC and GSC. The proposed approach ensures near-sinusoidal stator currents at the point of common coupling (PCC) under different load conditions [18]–[22], thereby enhancing overall power quality in DFIG-based wind energy systems connected to the grid. Compared to existing RSC–GSC harmonic mitigation schemes, the proposed approach integrates a multivariable filter with sliding mode control on both converters, enabling more robust suppression of multiple harmonic components under highly nonlinear and unbalanced load conditions. Unlike conventional PI-based methods or standalone APFs, our method ensures near-sinusoidal stator currents at the PCC without compromising active and reactive power control.

The remainder of this paper is organized as follows: Section 2 presents the system modeling, including the DFIG configuration and load representation under linear, nonlinear, balanced, and unbalanced conditions. Section 3 details the harmonic current identification methods and introduces the proposed mitigation strategies. Section 4 discusses the simulation setup and results, highlighting performance analysis and observed limitations. Finally, section 5 concludes the paper and outlines future research directions.

2. SYSTEM MODELING AND METHODOLOGY

2.1. Topology of the studied system

Currently, variable-speed wind systems based on the DFIG are the most widely used technology in onshore wind farms. Their main advantage lies in the fact that the static converters are sized for only a fraction of the nominal power of the DFIG, as they are connected to the grid through the rotor winding. The overall configuration of the studied system is illustrated in Figure 1. It consists of the wind energy conversion system that supplies various types of loads, including linear, non-linear, balanced, and unbalanced loads.

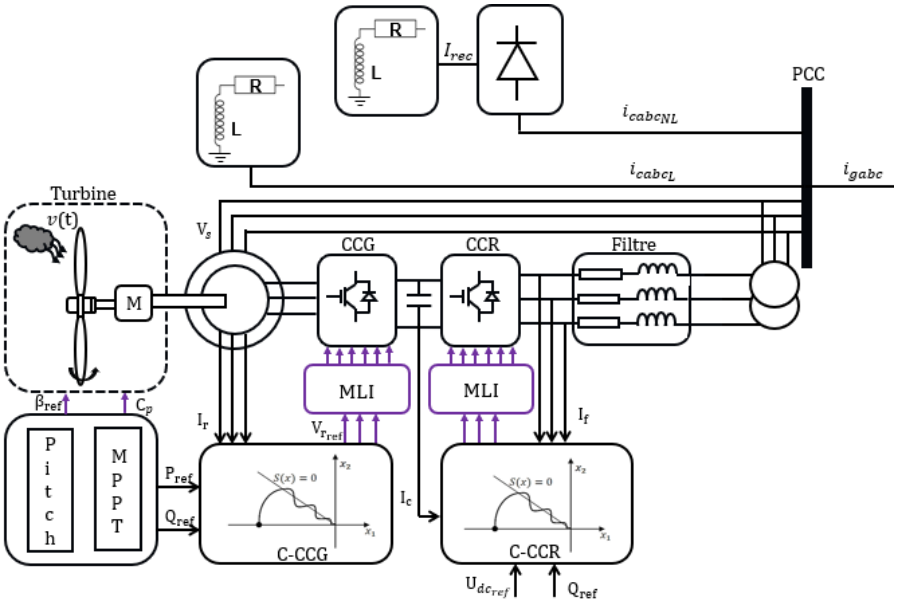

Figure 1. Block diagram of wind energie conversion system

2.2. DFIG modeling

Starting from the schematic representation of a DFIG in the reference frame of three phases, as widely presented in [23]–[26], and adopting the assumptions that the stator resistance R_s is negligible (which is reasonable for higher power levels) and that the stator flux φ_s is constant (assuming a constant stator voltage V_s) and oriented along the dq axis, the machine equations can be expressed as (1)–(4).

$$\begin{cases} V_{sd} = 0 \\ V_{sq} = V_s = \omega_s \varphi_s \\ V_{rd} = R_r I_{rd} + \dfrac{d\varphi_{rd}}{dt} - \omega_r \varphi_{rq} \\ V_{rq} = R_r I_{rq} + \dfrac{d\varphi_{rq}}{dt} + \omega_r \varphi_{rd} \end{cases} \tag{1}$$

and:

$$\begin{cases} \varphi_{sd} = \varphi_s = L_s I_{sd} + M I_{rd} \\ 0 = L_s I_{sq} + M I_{rq} \\ \varphi_{rd} = L_r I_{rd} + M I_{sd} \\ \varphi_{rq} = L_r I_{rq} + M I_{sq} \end{cases} \tag{2}$$

The stator currents are given by the following system, as (3).

$$\begin{cases} I_{sd} = \dfrac{\varphi_s}{L_s} - \dfrac{M}{L_s} I_{rd} \\ I_{sq} = -\dfrac{M}{L_s} I_{rq} \end{cases} \tag{3}$$

The active and reactive powers become (4).

$$\begin{cases} P_s = V_{sq} I_{sq} = -\dfrac{M}{L_s} V_s I_{rq} \\ Q_s = V_{sq} I_{sd} = \dfrac{V_s \varphi_s}{L_s} - \dfrac{M V_s}{L_s} I_{rd} \end{cases} \tag{4}$$

The previous equations describe the dynamic behavior of the DFIG under the assumptions of negligible stator resistance and constant stator flux oriented along the dq-axis. This mathematical model forms the foundation for analyzing the generator performance and its interaction with the electrical network. In practical applications, the DFIG supplies various types of load, which can be linear or nonlinear, balanced, or unbalanced. Accurate modeling of these loads is essential to evaluate their impact on power quality, particularly harmonic distortions. The next section presents the modeling approaches for the loads connected to the system.

2.3. Load modelling

Since wind turbines are connected to the distribution grid, they are often located close to polluting loads that inject harmonics into the network. The load is connected to the wind energy conversion system via the point of common coupling, as shown in Figure 1. Two types of loads are considered:

i) Linear loads: which may be inductive and/or resistive, consuming active and/or reactive power;
ii) Nonlinear loads: represented here by a three-phase diode bridge rectifier supplying a direct current (DC) load, which can also have inductive and resistive components.

If the load values are identical across the three phases, the load is considered balanced; otherwise, it is unbalanced. A preliminary test was conducted to validate the modeling of balanced and unbalanced loads. The corresponding current waveforms are shown in Figure 2. At time t = 500 ms, a variation in the active and reactive power of the loads is imposed in order to increase the THD, with the aim of highlighting the proposed solution for the converter system's contribution to harmonic mitigation.

To avoid overloading the article with figures, spectral results for all cases are summarized in Table 1, including THD and the percentage of the main harmonic components. The high value of the DC component is mainly due to the nonlinear nature of the load. As observed in Figure 2, a DC component appears in balanced and unbalanced load conditions, explains the asymmetry of the waveforms with respect to the time axis.

2.4. Simulation of the wind energy system in the presence of harmonic-polluting loads

To highlight the performance of the wind energy system in the presence of electrical loads, the simulation of the conversion system connected to the grid through the PCC was carried out. On the other side, the PCC is connected to harmonic-polluting loads, as illustrated in Figure 1. The simulations produced the results shown in Figure 3. The results of the spectra of the currents injected into the grid I_g are summarized in Table 2. Based on these results, it is observed that the presence of the wind energy system worsens the situation: in fact, the THD increases and the grid current becomes more distorted. Therefore, a filtering solution is essential.

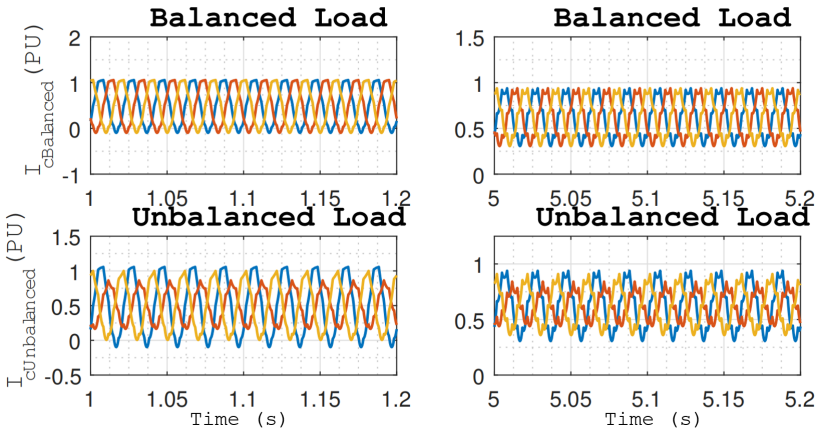

Figure 2. Three-phase current responses for balanced and unbalanced load cases

Table 1. Summary table of the THD of load currents

Frequency (Hz)	$I_{cbalanced}$		$I_{cunbalanced}$					
	t = 100 ms	t = 500 ms	t = 100 ms			t = 500 ms		
			I_{ca}	I_{cb}	I_{cc}	I_{ca}	I_{cb}	I_{cc}
0	86	217	86.88	154	104	217	386	2622
50	100	100	100	100	100	100	100	100
300	5.05	12.63	5.05	8.99	6.10	12.63	22.46	15.24
600	1.4	3.5	1.40	2.49	1.69	3.5	6.23	4.23
900	0.64	1.59	0.64	1.13	0.77	1.59	2.83	1.92
THD (%)	5.31	13.26	5.31	9.44	6.40	13.26	23.59	16

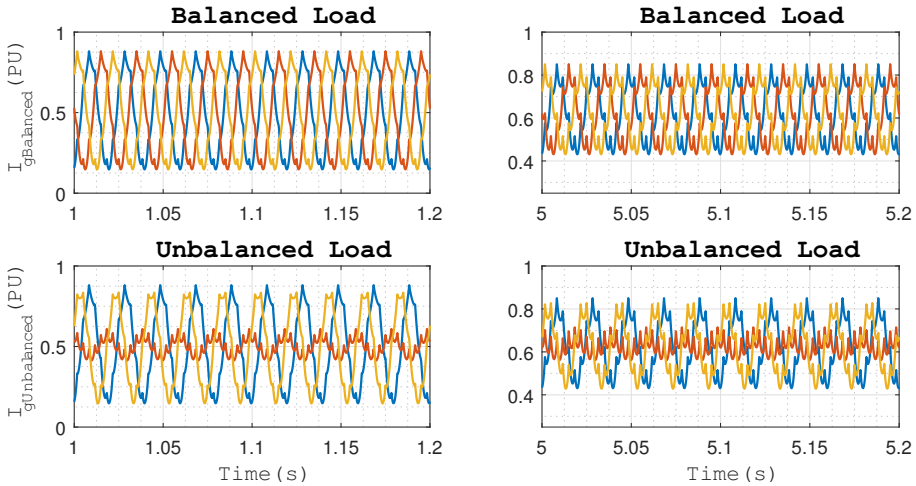

Figure 3. The currents injected into the grid to which the wind turbine and the loads are connected

Table 2. Summary table of the THD of load currents

Frequency (Hz)	$I_{gbalanced}$		$I_{gunbalanced}$					
	t = 100 ms	t = 500 ms	t = 100 ms			t = 500 ms		
			I_{ga}	I_{gb}	I_{gc}	I_{ga}	I_{gb}	I_{gc}
0	146.48	366.18	146	73.61	152.12	366.19	350	380
50	100	100	100	100	100	100	100	100
300	8.52	21.3	8.52	45.54	8.85	21.3	13.85	22.12
600	2.36	5.91	2.36	12.36	2.45	5.9	11.57	6.13
900	1.07	2.69	1.07	5.75	1.12	2.69	4.37	2.79
THD (%)	8.95	22.36	8.95	47.8	9.29	22.36	31.24	23.23

3. HARMONIC MITIGATION

When the wind energy system was connected to a distorted grid, the line current I_{gabc} exhibited harmonic frequency components of various orders, not limited to the 6th harmonic. In most previous studies, control strategies targeted only a single harmonic order, which was then used to modify the DFIG converter control. In contrast, the control strategy developed in this work considers all significant harmonic components present in the load current I_{cabc}. This comprehensive approach allows for a more accurate compensation under both balanced and unbalanced conditions.

3.1. Harmonic current identification

Several harmonic identification techniques have been reported in the literature. The most classical one, widely used in active power filter control, is the instantaneous power (PQ) theory, originally proposed by Akagi. It is based on the Concordia transformation, applied to phase-to-neutral voltages V_{sabc} and load currents, to compute instantaneous active and reactive powers. These powers can be decomposed as (5).

$$\begin{cases} P = \overline{P} + \widetilde{P} \\ Q = \overline{Q} + \widetilde{Q} \end{cases} \tag{5}$$

The DC components $\overline{P}$ and $\overline{Q}$ correspond to the fundamental components and are extracted using low-pass filters. The AC parts $\widetilde{P}$ and $\widetilde{Q}$ are then obtained by subtracting these DC components, allowing the harmonic currents generated by nonlinear loads to be identified.

Another widely used technique is based on the synchronous reference frame (SRF) method, introduced by Bhattacharya and illustrated in [27]. Like the PQ method, it begins with the Concordia transformation applied to the load currents, followed by a Park transformation that projects them onto the rotating dq frame. In this frame, the fundamental component appears as a DC term, while harmonic components manifest as AC terms. A simple band-pass filter can then isolate the fundamental component. The SRF method presents several advantages: it is immune to voltage harmonics and requires only two current sensors to identify all harmonic components of the nonlinear load. However, in its classical form, it does not permit the extraction of a specific harmonic order. In this work, a multi-variable filter (MVF) is employed for harmonic extraction, as described in [14]. The MVF enables the isolation of either the complete harmonic spectrum or a specific harmonic order, including both direct and inverse sequence components. Its transfer function is expressed as (6).

$$H(s) = \frac{Y_s}{Y_e} = \frac{ks + k^2 + j\omega_c}{s^2 + 2ks + k^2 + \omega_c^2} \tag{6}$$

Where: ω_c: characteristic pulsation of the filter (corresponding to the targeted frequency); k: positive constant controlling bandwidth and selectivity; Y_e: input signal to be filtered; and Y_s: output signal filtered at the selected frequency.

The cutoff angular frequency of the filter, denoted ω_c, is defined as (7).

$$\omega_c = \varepsilon n \omega_f \tag{7}$$

Where n represents the order of the signal component to be filtered, ε characterizes the type of component (direct or inverse), and K is a positive constant.

A Bode diagram of the selective filter was generated to analyze the effect of different values of the parameter K. It can be observed that increasing K reduces the filter's selectivity, resulting in a wider

bandwidth. In this case, instead of obtaining a signal containing a single frequency, the filtered signal exhibits additional components, introducing noise. However, the dynamic response of the overall system must also be considered, particularly regarding the stability of the system. According to Fourier's theory, any periodic signal can be expressed as a sum of sinusoidal components at multiples of its fundamental frequency. To isolate harmonics, it suffices to remove the fundamental component. Based on frequency analysis of the current from balanced loads (see Table 1), and neglecting harmonics above 1 kHz, the current in phase a can be expressed as (8).

$$I_c(t) = A_0 + A\sin(2\omega t + \varphi_1) + A_1\sin(12\omega t + \varphi_2) + A_2\sin(24\omega t + \varphi_3) + A_3\sin(36\omega t + \varphi_4) \quad (8)$$

After removing the fundamental component, the harmonic current becomes (9).

$$I_{c_{\text{har}}}(t) = A'_0 + A'_1\sin(12\omega t + \varphi_2) + A'_2\sin(24\omega t + \varphi_3) + A'_3\sin(36\omega t + \varphi_4) \quad (9)$$

3.2. Proposed harmonic mitigation strategies

Two complementary harmonic mitigation strategies have been considered for DFIG-based wind energy systems supplying nonlinear loads. Both approaches have been individually tested and evaluated in previous works. In this study, a third strategy is proposed as a combination of the two, aiming to enhance overall performance:

i) RSC-based compensation: In this approach, RSC control is modified by injecting specific harmonic components into rotor current reference, thereby reducing their propagation into stator current [14], [15].
ii) FSC-based active filtering: Here, the the full-scale converter (FSC) operates as an active filter that extracts and compensates for the harmonic components present in the measured grid currents [13], [16].
iii) Combined adaptive strategy: This enhanced method merges the advantages of the previous two. It introduces an adaptive adjustment block that ensures the DFIG maintains its primary objectives—active and reactive power control—while achieving improved harmonic mitigation [23], [24].

3.2.1. RSC control modification for harmonic current injection

Different control techniques can be applied to power converters. Among them, PI-based control remains the most commonly used due to its simplicity, whereas advanced nonlinear techniques such as backstepping or sliding mode control provide superior performance in terms of dynamic response and power quality. In this work, sliding mode control is applied to both converters, as extensively developed in [23], [24]. Based on the mathematical models of the generator, DC bus, and grid filter, control laws have been derived to manage both the RSC and the GSC. The RSC controller is mainly responsible for ensuring that the active and reactive powers follow their respective references. In the modified version of the RSC control, the same fundamental control structure is preserved, but an additional term is introduced to eliminate the 6th-order harmonic. This is achieved by injecting the corresponding harmonic current into the rotor current reference used within the control loop. According to the DFIG model presented in the modeling section, under stator flux orientation (aligned with the d-axis), active and reactive power control requires computing the rotor current, see in (4), from which the voltage references are derived. In steady-state operation, the DFIG inherently couples the stator and rotor currents, acting as a current amplifier. Consequently, the harmonic components present in the load are not only incorporated into the control strategy but also amplified to effectively compensate for the harmonic distortion observed at the point of renewable resources (PRR). The harmonic components of the rotor current references are obtained as (10).

$$\begin{cases} i_{rdh} = \dfrac{L_s}{M \cdot L_m} i_{cdh} \\ i_{rqh} = \dfrac{L_s}{M \cdot L_m} i_{cqh} \end{cases} \quad (10)$$

Thus, the full expressions of the rotor current references are given by (11).

$$\begin{cases} I_{rq}^{\text{ref}} = -\dfrac{L_s V_s \cdot M \cdot P_s^{\text{ref}}}{L_s M \cdot L_m} + i_{cqh} \\ I_{rd}^{\text{ref}} = \dfrac{V_s}{\omega_s \cdot M} - \dfrac{L_s V_s \cdot M \cdot Q_s^{\text{ref}}}{L_s M \cdot L_m} + i_{cdh} \end{cases} \quad (11)$$

Once these updated rotor current references are computed, the corresponding reference voltages are obtained using (1), as in the standard control structure. These voltages are then applied to the RSC, which is controlled through pulse width modulation (PWM). Through this modification, the RSC actively cancels the 6th-order harmonic component of the load current, as illustrated in Figure 4.

The presence of harmonic components in the rotor voltage can significantly affect the DFIG's internal behavior. According to (1), these harmonics generate corresponding harmonic currents in the rotor circuit, which can then propagate to the stator side. The frequency and sequence of these harmonics are defined by (3). Consequently, the induced imbalance between rotor and stator currents can lead to nonuniform magnetic loading, resulting in localized magnetic saturation, excessive heating, and increased copper and iron losses. These effects ultimately reduce the overall efficiency and operational lifetime of the DFIG. Furthermore, according to (4), the mismatch between the generated and reference power components may indicate a loss of tracking accuracy in the initial control structure. To mitigate these effects and maintain power control precision, a refinement of the rotor current references is therefore required.

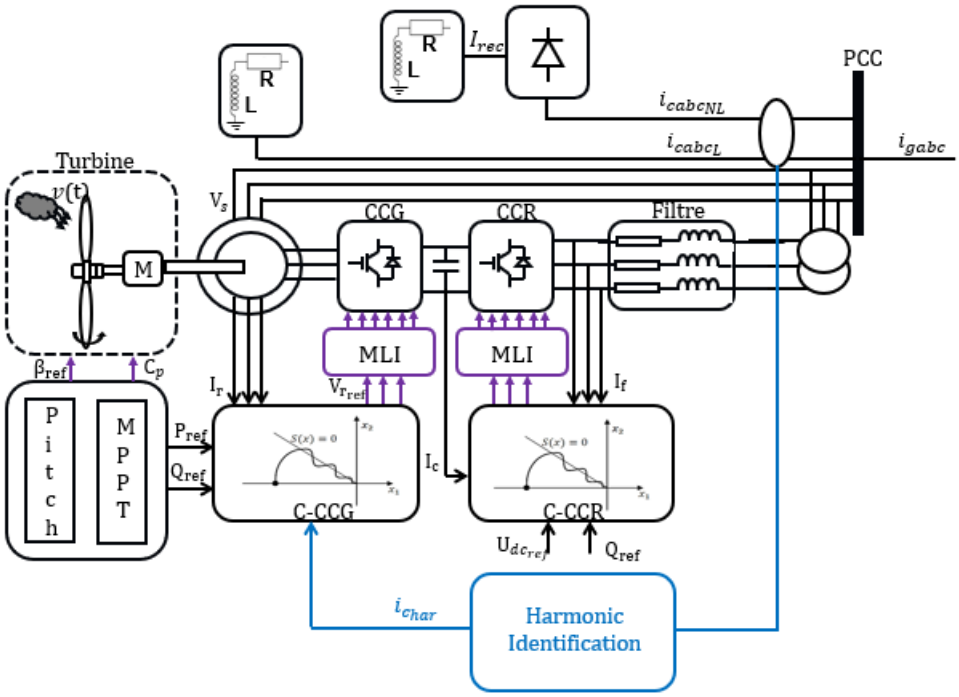

Figure 4. Modified RSC control via sliding mode for harmonic mitigation

3.2.2. FSC-based active filtering for harmonic compensation

The second harmonic mitigation strategy relies on a dedicated active filter (AF) implemented through a shunt converter, the full-scale converter (FSC), which has a structure similar to the RSC and GSC used in the DFIG-based wind energy conversion system as illustrated in Figure 1. The main distinction lies in the control technique. While the RSC and GSC are driven by PWM, the FSC is controlled using a hysteresis current control method. This enables rapid and precise tracking of the harmonic components extracted from the load current. The FSC is connected in parallel with the load and is exclusively responsible for compensating the isolated harmonic components obtained using the harmonic extraction method described earlier. By injecting the appropriate compensating currents into the grid, this approach effectively reduces the THD at the PCC. The FSC-based active filtering is particularly efficient in mitigating multiple harmonic orders simultaneously and dynamically adapts to variations in load conditions. It ensures harmonic compensation without affecting the primary active and reactive power delivered by the DFIG.

3.2.3. Combined generator-and grid-side harmonic mitigation

The combined strategy merges the two previously discussed approaches. The RSC is modified to inject harmonic components directly into the rotor current reference, while a parallel FSC-based active filter simultaneously injects compensating currents into the grid (Figure 5). This dual-action strategy allows harmonics to be mitigated at two levels: internally through the generator control and externally via the active filter. Such an approach enhances overall harmonic suppression and ensures that the DFIG's primary objectives—active and reactive power regulation—are maintained.

3.2.4. Enhanced method of the RSC modification

The adapted control strategy must ensure harmonic current mitigation while maintaining the active power control of the DFIG. It is essential to emphasize that harmonic compensation should never compromise the active power output of the wind turbine, especially under favorable wind conditions that allow for nominal power generation. Therefore, a modification of the rotor current references is implemented at the RSC level, prioritizing the regulation of active power production. The core idea lies in limiting the reference currents according to the flowchart illustrated in Figure 6, which ensures that harmonic compensation remains effective without degrading the primary function of the wind energy conversion system.

The rotor currents are first calculated at their maximum values. The harmonic currents of the rotor are then analyzed to determine the reference currents, which are used to calculate the reference voltages of the modulator's pulse width. The adjustment mechanism is illustrated in Figure 7. Blocks 1 and 2 illustrated in Figure 7 are composed as (12)–(14).

$$V_{CCGq\text{-}Equi} = -\frac{L_s L_{r\sigma}}{MV_s}\dot{P}_s^{\text{ref}} + R_r I_{rq} + g\,\omega_s L_r \sigma I_{rd} + g\,\frac{MV_s}{L_s} \tag{12}$$

$$V_{CCGd\text{-}Equi} = L_r\sigma\left(\frac{V_s}{\omega_s M} - \frac{L_s}{V_s M}\dot{Q}_s^{\text{ref}}\right) + R_r I_{rd} - g\,\omega_s L_r \sigma I_{rq} \tag{13}$$

$$V_{CCGq} = -\frac{L_s L_{r\sigma}}{MV_s}\dot{P}_s^{\text{ref}} + R_r I_{rq} + g\,\omega_s L_r \sigma I_{rd} + g\,\frac{MV_s}{L_s} + L_r\sigma v_1\,\text{sgn}(s(P)) \tag{14}$$

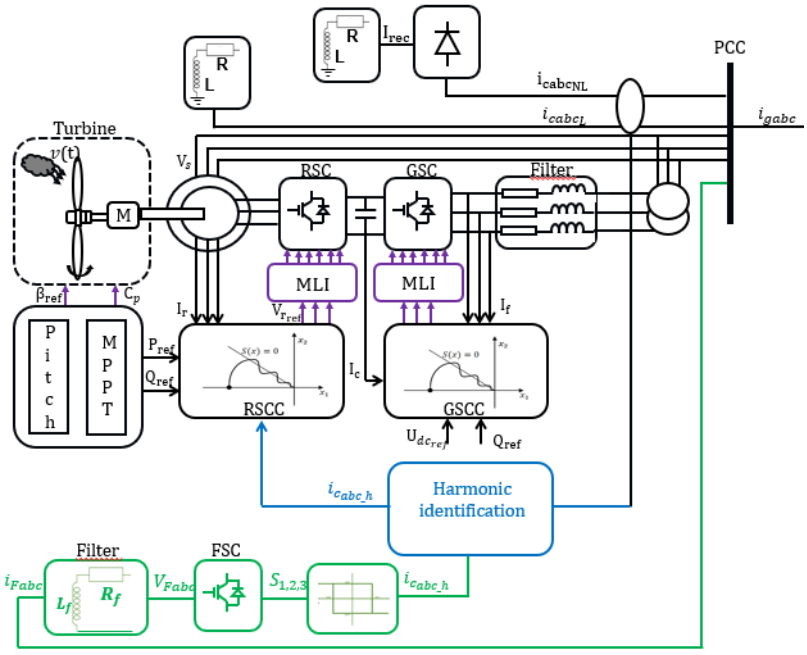

Figure 5. Combined RSC and FSC-based harmonic mitigation for a DFIG system

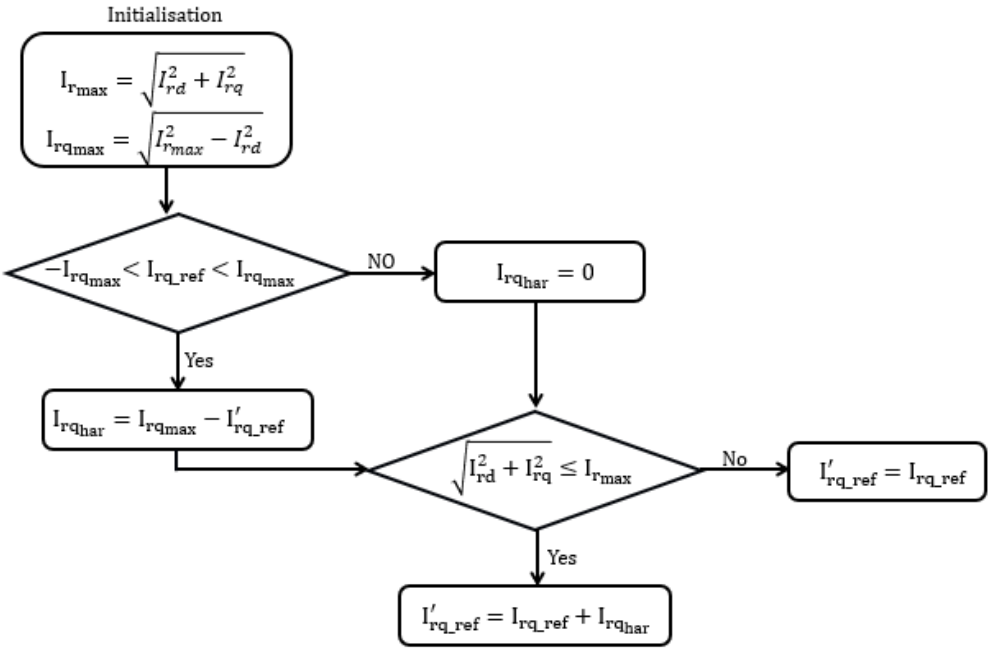

Figure 6. Flowchart of the reference current adjustment

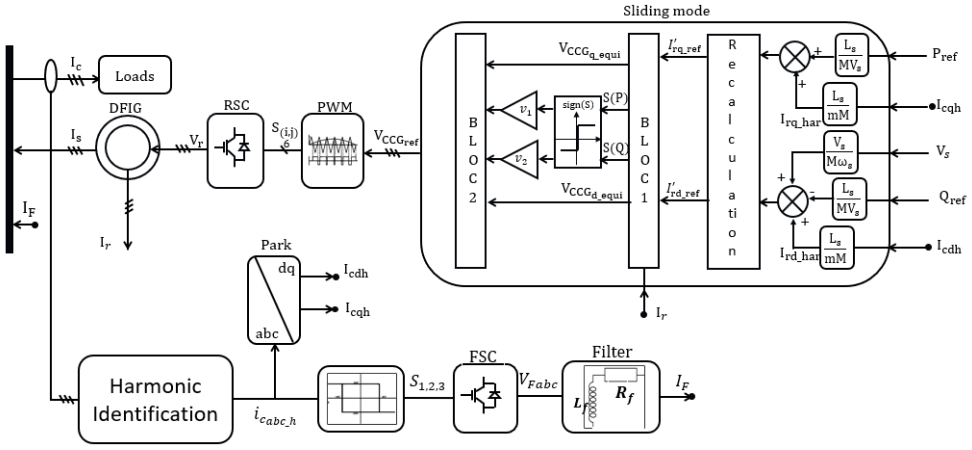

Figure 7. Block diagram of the modified RSC for harmonic mitigation integrating the current reference recalculation block

4. EVALUATION OF THE CONTROL STRATEGY

4.1. Simulation results

The simulations were conducted to evaluate the validity and effectiveness of the proposed control strategy. A 1.5 MW DFIG model was developed in MATLAB/Simulink. Regarding the load conditions, both balanced and unbalanced loads are considered. Before 500 ms, the linear load consumes 500 kW of active power and 800 kVAR of reactive power, while the nonlinear load absorbs 90 kW and 1.2 MVAR. After 500 ms, the linear load remains unchanged with 500 kW and 800 kVAR, whereas the nonlinear load increases to 500 kW and 3 MVAR. To isolate the influence of harmonic mitigation and clearly observe the control dynamics, the system was simulated under fixed wind speed conditions. This approach eliminates additional harmonics that could arise from wind speed fluctuations. The simulation duration was set to 600 ms and included both balanced and unbalanced load scenarios. In each case, linear and nonlinear loads were applied. A step change in active and reactive power was also introduced to increase the THD and evaluate the control system's robustness.

4.2. Discussion of results

To streamline the analysis and emphasize the performance of the proposed strategy, the discussion focuses on the THD of key currents (I_r, I_s, I_c, and I_g) under the most severe condition—unbalanced loading. The simulation results yielded the current waveforms shown in Figure 8, while the active and reactive power profiles are presented in Figures 9 and 10. Figure 11 illustrates the DC-link voltage, which remains stable throughout the simulation, confirming the proper energy balance and robustness of the proposed control scheme. Table 3 summarize the spectral analysis THD of the three-phase currents.

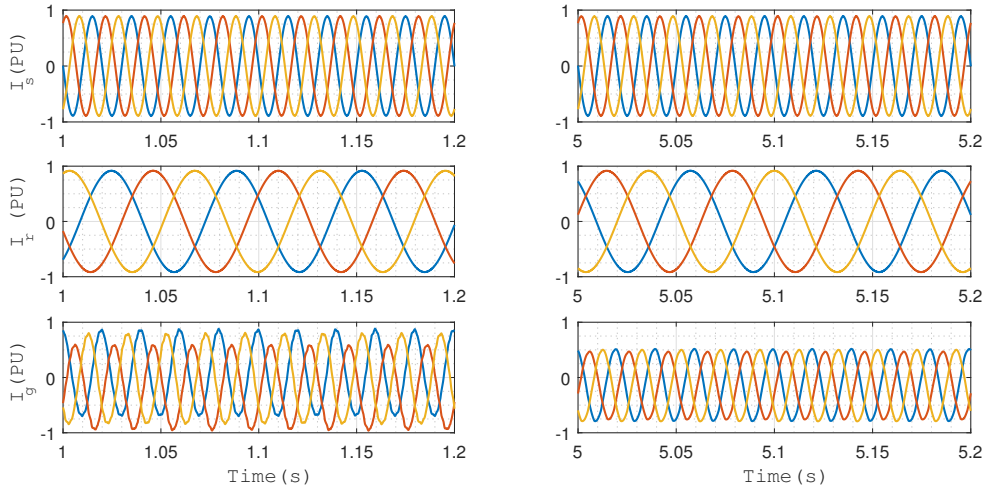

Figure 8. The currents of WECS under unbalanced load with adjustment block

Similar to the previously proposed method, harmonic compensation is successfully achieved. However, the major improvement introduced by the adjustment block lies in preserving the primary energy conversion function of the wind system. Figures 9 and 10 show that the active power accurately follows its reference derived from the mechanical subsystem. Moreover, the rotor currents remain undistorted even under unbalanced load conditions, thus preventing potential operational issues in the DFIG.

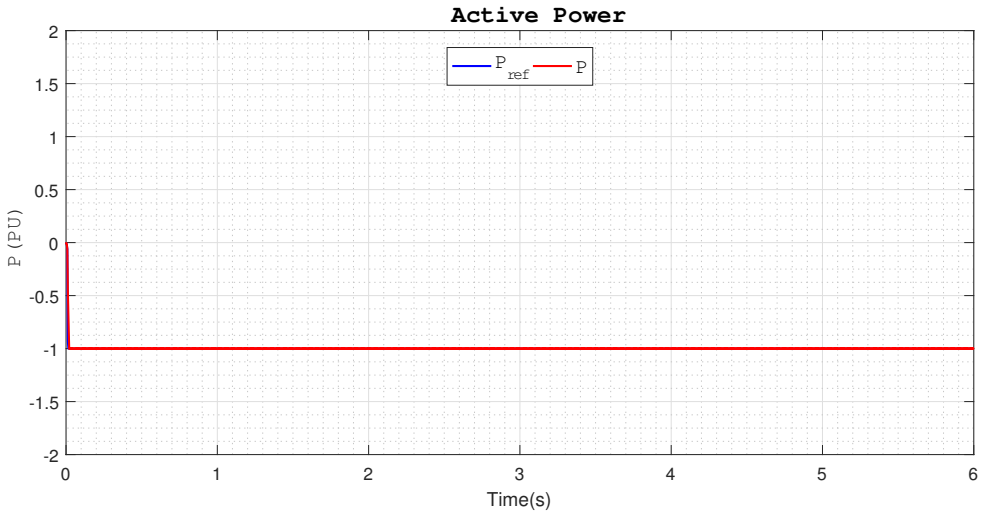

Figure 9. The active power of WECS under unbalanced load with adjustment block

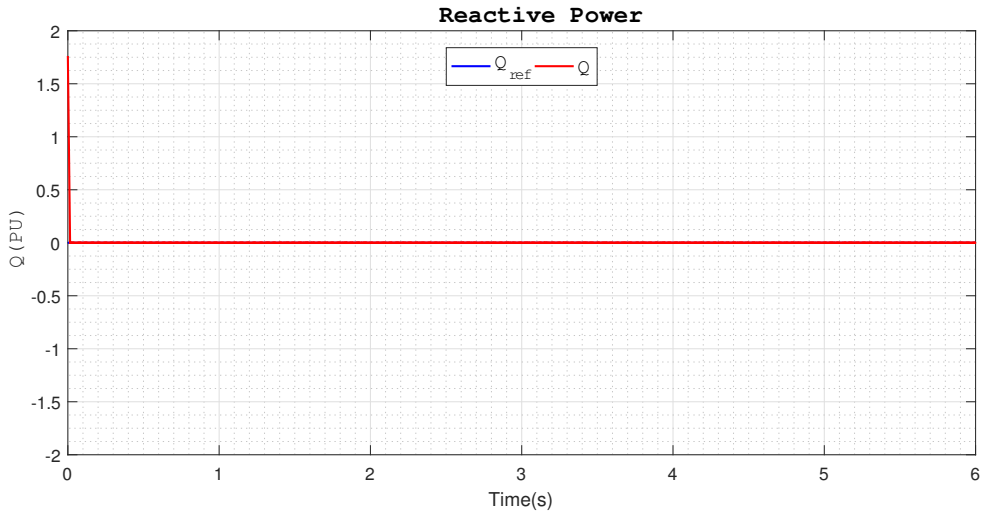

Figure 10. The reactive power of WECS under unbalanced load with adjustment block

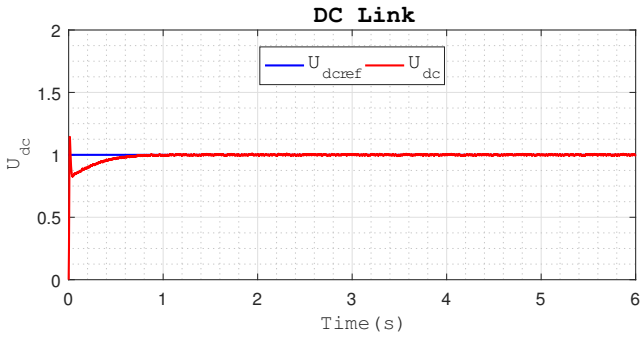

Figure 11. The DC link voltage of WECS under unbalanced load

Table 3. Spectral analysis of the three-phase currents under unbalanced load conditions

THD	First phase				Second phase				Third phase			
	I_c	I_s	I_r	I_g	I_c	I_s	I_r	I_g	I_c	I_s	I_r	I_g
t = 180 ms	5.31	0.03	0.04	4.55	9.44	0.03	0.03	3.05	6.40	0.03	0.03	3.71
t = 580 ms	13.26	0.03	0.04	1.39	23.59	0.03	0.04	1.48	16.00	0.03	0.04	1.41

5. CONCLUSION

This article presented and analyzed three control strategies to enhance the current quality injected by a DFIG-based wind energy conversion system (WECS) operating under unbalanced and nonlinear load conditions that typically cause significant harmonic distortion. The first method modified the RSC control, the second introduced an additional converter dedicated to harmonic mitigation, and the third combined both strategies into a unified scheme. Simulation results confirmed that the combined approach achieves a substantial reduction in THD—for instance, lowering the grid current THD from 31.24 to lower than 5% under unbalanced nonlinear load conditions. Moreover, the improved design preserved the DFIG's primary function by maintaining accurate active power tracking and stable DC-link voltage, while also mitigating electromagnetic stress on the generator. The main contribution of this study lies in demonstrating that coordinated RSC and FSC control can simultaneously ensure harmonic compensation and power quality without sacrificing energy conversion efficiency. However, this work was limited to simulations under fixed wind speed and specific load scenarios. Future research will focus on extending the strategy to variable wind profiles, dynamic load conditions, and real-time hardware validation (implementing the proposed controller on

DSP or FPGA platforms), in order to further assess the robustness and practical implementation of the proposed control scheme. The variation of the DFIG's internal parameters, as well as network disturbances (voltage dip), could also constitute future research directions to test and confirm the robustness of the control strategy.

FUNDING INFORMATION

This research did not receive any specific external funding. The article processing charges and publication expenses were supported by the authors' affiliated institution.

AUTHOR CONTRIBUTIONS STATEMENT

This journal uses the Contributor Roles Taxonomy (CRediT) to recognize individual author contributions, reduce authorship disputes, and facilitate collaboration.

Name of Author	C	M	So	Va	Fo	I	R	D	O	E	Vi	Su	P	Fu
Hind Elaimani	✓	✓	✓	✓	✓	✓	✓	✓	✓	✓	✓		✓	✓
Noureddine Elmouhi	✓			✓			✓			✓		✓		

C : **C**onceptualization
M : **M**ethodology
So : **So**ftware
Va : **Va**lidation
Fo : **Fo**rmal Analysis
I : **I**nvestigation
R : **R**esources
D : **D**ata Curation
O : Writing - **O**riginal Draft
E : Writing - Review & **E**diting
Vi : **Vi**sualization
Su : **Su**pervision
P : **P**roject Administration
Fu : **Fu**nding Acquisition

CONFLICT OF INTEREST STATEMENT

The authors state no conflict of interest with respect to the research, authorship, and publication of the article.

DATA AVAILABILITY

The authors confirm that the data supporting the findings of this study are available on request from the corresponding author.

REFERENCES

[1] K. Daniel, L. Kütt, M. N. Iqbal, N. Shabbir, H. A. Raja, and M. U. Sardar, "A review of harmonic detection, suppression, aggregation, and estimation techniques," *Applied Sciences (Switzerland)*, vol. 14, no. 23, 2024, doi: 10.3390/app142310966.

[2] T. Abdelwahed, M. Radouane, T. Abderrahim, M. Aboulfatah, and R. Nabila, "Comparative study between fast terminal and second order sliding mode controls applied to a wind energy conversion system," *Indonesian Journal of Electrical Engineering and Computer Science*, vol. 22, no. 2, pp. 765–779, 2021, doi: 10.11591/ijeecs.v22.i2.pp765-779.

[3] Z. Reguieg, I. Bouyakoub, and F. Mehedi, "Harmonic mitigation in grid-integrated renewable energy systems with nonlinear loads," *Energy*, vol. 324, 2025, doi: 10.1016/j.energy.2025.135882.

[4] H. Mendonça, R. M. de Castro, S. Martínez, and D. Montalbán, "Voltage impact of a wave energy converter on an unbalanced distribution grid and corrective actions," *Sustainability (Switzerland)*, vol. 9, no. 10, 2017, doi: 10.3390/su9101844.

[5] X. Liang and C. Andalib-Bin-Karim, "Harmonics and mitigation techniques through advanced control in grid-connected renewable energy sources: a review," *IEEE Transactions on Industry Applications*, vol. 54, no. 4, pp. 3100–3111, 2018, doi: 10.1109/TIA.2018.2823680.

[6] A. Bouhouta, S. Moulahoum, and N. Kabache, "Harmonic mitigation in utility grid with highly unbalanced nonlinear load using intelligent controller: an experimental study," *Przeglad Elektrotechniczny*, no. 4, pp. 1–7, 2022, doi: 10.15199/48.2022.04.1.

[7] A. Mishra, P. M. Tripathi, and K. Chatterjee, "A review of harmonic elimination techniques in grid connected doubly fed induction generator based wind energy system," *Renewable and Sustainable Energy Reviews*, vol. 89, pp. 1–15, 2018, doi: 10.1016/j.rser.2018.02.039.

[8] A. Mishra and K. Chatterjee, "Harmonic analysis and attenuation using LCL-filter in doubly fed induction generator based wind conversion system using real time simulation based OPAL-RT," *Alexandria Engineering Journal*, vol. 61, no. 5, pp. 3773–3792, 2022, doi: 10.1016/j.aej.2021.08.079.

[9] V. T. Phan and H. H. Lee, "Control strategy for harmonic elimination in stand-alone DFIG applications with nonlinear loads," *IEEE Transactions on Power Electronics*, vol. 26, no. 9, pp. 2662–2675, 2011, doi: 10.1109/TPEL.2011.2123921.

[10] J. Amini, "Disturbances rejection and harmonics reduction of doubly fed induction generator based wind energy conversion systems," *Electric Power Components and Systems*, vol. 40, no. 13, pp. 1423–1444, 2012, doi: 10.1080/15325008.2012.700381.

[11] K. V. Bhadane, M. S. Ballal, A. Nayyar, D. P. Patil, T. H. Jaware, and H. P. Shukla, "A comprehensive study of harmonic pollution in large penetrated grid-connected wind farm," *Mapan - Journal of Metrology Society of India*, vol. 36, no. 4, pp. 729–749, 2021, doi: 10.1007/s12647-020-00407-z.
[12] E. Guest, K. H. Jensen, and T. W. Rasmussen, "Mitigation of harmonic voltage amplification in offshore wind power plants by wind turbines with embedded active filters," *IEEE Transactions on Sustainable Energy*, vol. 11, no. 2, pp. 785–794, 2020, doi: 10.1109/TSTE.2019.2906797.
[13] M. Reddak, A. Berdai, A. Gourma, and J. Boukherouaa, "An improved control strategy using RSC of the wind turbine based on DFIG for grid harmonic currents mitigation," *International Journal of Renewable Energy Research*, vol. 8, no. 1, pp. 266–273, 2018, doi: 10.20508/ijrer.v8i1.6726.g7300.
[14] A. Gaillard, P. Poure, and S. Saadate, "Active filtering capability of WECS with DFIG for grid power quality improvement," *IEEE International Symposium on Industrial Electronics*, pp. 2365–2370, 2008, doi: 10.1109/ISIE.2008.4676984.
[15] M. T. Abolhassani, P. Enjeti, and H. A. Toliyat, "Integrated doubly-fed electric alternator/active filter (IDEA), a viable power quality solution, for wind energy conversion systems," *Conference Record - IAS Annual Meeting (IEEE Industry Applications Society)*, vol. 3, pp. 2036–2043, 2004, doi: 10.1109/ias.2004.1348747.
[16] A. K. Jain and V. T. Ranganathan, "Wound rotor induction generator with sensorless control and integrated active filter for feeding nonlinear loads in a stand-alone grid," *IEEE Transactions on Industrial Electronics*, vol. 55, no. 1, pp. 218–228, 2008, doi: 10.1109/TIE.2007.911196.
[17] M. Boutoubat, L. Mokrani, M. MacHmoum, and F. Auger, "Selective harmonics compensation using a WECS equipped by a DFIG," *IECON Proceedings (Industrial Electronics Conference)*, pp. 745–750, 2012, doi: 10.1109/IECON.2012.6388658.
[18] B. Sabir, V. K. Rawat, M. Faizan, and M. Tahir, "Analysis of generated harmonics in DFIG driven by wind turbine during linear non-linear load," *2021 International Conference on Computer Communication and Informatics, ICCCI 2021*, 2021, doi: 10.1109/ICCCI50826.2021.9402269.
[19] S. S. Das and U. Rajkiran, "Harmonic mitigation in wind energy conversion," *International Journal of Electrical, Electronics and Data Communication 2*, no. 9, 2014.
[20] F. S. Dos Reis, S. Islam, K. Tan, J. V. Alé, F. D. Adegas, and R. Tonkoski, "Harmonic mitigation in wind turbine energy conversion systems," *PESC Record - IEEE Annual Power Electronics Specialists Conference*, 2006, doi: 10.1109/PESC.2006.1712186.
[21] S. S. Das, S. C. Gupta, and S. K. Bhargava, "Harmonic reduction methods for wind energy conversion systems: A review," *2014 IEEE Students' Conference on Electrical, Electronics and Computer Science*, SCEECS 2014, 2014, doi: 10.1109/SCEECS.2014.6804487.
[22] R. Kumar and C. Gupta, "Methods for reducing harmonics in wind energy conversion systems: a review," *Research Journal of Engineering Technology and Medical Sciences*, vol. 4, no. 2, 2021.
[23] H. Elaimani, A. Essadki, N. Elmouhi, and R. Chakib, "The active and reactive powers' control of the DFIG during variations of its parameters," *Proceedings of 2018 6th International Renewable and Sustainable Energy Conference, IRSEC 2018*, 2018, doi: 10.1109/IRSEC.2018.8702951.
[24] H. Elaimani, A. Essadki, N. Elmouhi, and R. Chakib, "Comparative study of the grid side converter's control during a voltage dip," *Journal of Energy*, vol. 2020, pp. 1–11, 2020, doi: 10.1155/2020/7892680.
[25] Y. Djeriri, "Commande directe du couple et des puissances d'une MADA associée a un système éolien par les techniques de l'intelligence artificielle," Université de Constantine, 2015.
[26] T. Ghennam, "Supervision d'une ferme éolienne pour son intégration dans la gestion d'un réseau électrique, Apports des convertisseurs multi niveaux au réglage des éoliennes à base de machine asynchrone à double alimentation," Université de Grenoble, 2011.
[27] A. Gaillard, "Système éolien basé sur une MADA: contribution à l'étude de la qualité de l'énergie électrique et de la continuité de service," Université Henri Poincaré, 2010. [Online]. Available: https://www.researchgate.net/publication/324494619.

BIOGRAPHIES OF AUTHORS

Hind Elaimani was born in Marrakesh, Morocco in 1988. She is currently a professor and research professor at the electrical engineering department of ISGA - Rabat. In 2022, she received her Ph.D. degree from ENSIAS Mohammed V University Morocco. In 2011, she received the Master Degree in Electrical Engineering, from sciences and technologies Faculty (FST), Marrakesh, Morocco. Her current research interests include renewable energy, motor drives, and power system. She can be contacted at email: h.elaimani@gmail.com.

Noureddine Elmouhi was born in Marrakesh, Morocco in 1987. He is currently a professor and research professor at the electrical engineering department of ISGA - Rabat. In 2022, he received his Ph.D. degree from ENSIAS Mohammed V University Morocco. He received the Engineer Degree in Electrical Engineering, from sciences and technologies Faculty (FST), Marrakesh, Morocco, in 2010. His research focuses primarily on the design, modeling, and development of advanced control techniques applied to renewable energy-based power generation systems. He can be contacted at email: n.elmouhi@gmail.com.